Separation of Binary Solvent Mixtures with Solvent Resistant Nanofiltration Membranes Part B: Process Modeling

Journal:	*RSC Advances*
Manuscript ID:	RA-ART-05-2014-004224.R1
Article Type:	Paper
Date Submitted by the Author:	16-Jul-2014
Complete List of Authors:	Li, Jiandong; Beijing University of Chemical Technology, Wang, Miaomiao; b. College of Life Science and Technology, Huang, Yucui; a. State Key Laboratory of Chemical Recourse Engineering, Luo, Beibei; State Key Laboratory of Chemical Recourse Engineering, Zhang, Yuan; State Key Laboratory of Chemical Recourse Engineering, Yuan, Qipeng; State Key Laboratory of Chemical Recourse Engineering,

Separation of Binary Solvent Mixtures with Solvent Resistant Nanofiltration Membranes

Part B: Process Modeling

Jiandong Li[a*], Miaomiao Wang[b], Yucui Huang[a], Beibei Luo[a], Yuan Zhang[a], Qipeng Yuan[a]

a. State Key Laboratory of Chemical Recourse Engineering, Beijing University of Chemical Technology, Beijing, 100029, PR China.

b. College of Life Science and Technology, Beijing University of Chemical Technology, Beijing, 100029, PR China.

[*]Email: jandorlee@hotmail.com,

Telephone: 0086-10-64437610,

Fax: 0086-10-64437610

Abstract

This Part B of a two paper series develops an improved model derived from the classical solution-diffusion model, specifically for solvent separation process in SRNF. Important assumptions for this process from the first part of this work were adopted and only two parameters, i.e. the Hansen solubility parameter and dielectric constant, were integrated in this model. Separation factors of DuraMem^{TM} 150, 200, 300 and MPF-44 fitted well with this new model and that of DuraMem^{TM} 500 and DuraMem^{TM} 900 had a poor correlation, which was consistent with the author's hypotheses. This model provides a new approach to understand solvent separation processes in SRNF, and offers a good breakthrough point for further work in this field.

Key words: solvent separation; modeling; solubility parameter; dielectric constant; nanofiltration

1. Introduction

SRNF is a new burgeoning technology that is able to separate mixtures down to a molecular level, and its applications have been expanded in food chemistry, petrochemistry, catalysis, pharmaceutical manufacturing, etc [1]. Due to its promising energy- and waste-efficient advantages, a few researchers have attempted to explore SRNF's potential in separating solvent mixtures [2-4]. An interesting discovery has been reported in part A of this work corresponding to the transport of ethanol/hexane through DuraMem^{TM} 150, the separation factor of which is about 6. In this part a model predicting the mass transfer has been developed based on the solution-diffusion mechanism. However, before introducing the new model, existing models based on the solution-diffusion mechanism in SRNF will be briefly reviewed first in order to better understand the solvent transport process.

Some models, like the resistance-in-series, solution-diffusion, solution diffusion with imperfection (SDI) or combination of them, have been built to describe solvent transport in SRNF so far [5-15]. Within these existing models, only models based on the solution-diffusion mechanism will be introduced, since in the first part it was demonstrated that the mass transfer should be a typical solution-diffusion one to achieve separation. Within these solution-diffusion based models, Bhanushali et al. [6] firstly presented a valuable one to describe the solvent flux of SRNF membranes, as Equation (1) and (2) shows.

$$J_{solvent} \propto A \tag{1}$$

$$A \propto \left(\frac{v_m}{\mu}\right)\left(\frac{1}{\phi^n \gamma_{sv}}\right) \tag{2}$$

In these two equations, A is the solvent permeability coefficient, including both the diffusivity and solubility parts in the classical form of the Solution-diffusion model [16]. Four measurable physical properties, v_m, μ, ϕ^n and γ_{sv}, representing the solvent molar volume, solvent viscosity, a sorption value of solvent in the membrane and surface energy of the membrane, respectively, were included in their proposed model. Although a high correlation was found between the model and their experimental data, some questions were hard to answer. Firstly, a higher value of ϕ^n implies that the membrane and solvent have a high affinity, and a high flux should be expected. Moreover, for polar solvents, a high value of γ_{sv} still indicates strong interactions between the membrane and solvent and accordingly a better permeation should be available. Contradictorily, both of these two parameters were put on the denominator, which is obvious hard to explain. Yet, as the model firstly introduced the solution-diffusion mechanism in SRNF, it was quite instructive.

Another significant model based on the solution-diffusion mechanism was developed by Geens et al. [7] in Equation (3) and (4).

$$J_{solvent} \propto A \tag{3}$$

$$A \propto \left(\frac{v_m}{\mu \Delta_\gamma}\right) \tag{4}$$

This model revised Bhanushali's, and still kept the solvent molar volume v_m and solvent viscosity μ. The defective parameters, ϕ^n and γ_{sv}, were however removed from this model, and at the same time a new parameter Δ_γ, denoting the difference in surface tension between the solid membrane material and the liquid solvent, was integrated. This semi-empirical model was in good correlation with their experimental data, and provided valuable suggestions for later research [8, 9].

Atsushi et al. [10] proposed a model combining the regular solution model with the solution-diffusion model to describe the permeability of a PDMS-based dense membrane for binary solvent-hexane and diesel fuel-kerosene systems, and the model is shown in Equation (5).

$$J_{solvent} = [D(\Delta p - \Delta\pi)/\lambda^2]exp\left[-{\phi_{mem}}^2(V_m(\sigma_{mem} - \delta_s)^2/RT)\right] \quad (5)$$

This equation captures many important factors for permeability such as D for diffusion coefficient, $\Delta\pi$ for osmotic pressure, λ for membrane thickness, ϕ_{mem} for volume fraction of membrane polymer in membrane phase, V_m for molar volume of solvent and σ_s for solvent solubility parameter. The model fitted well with the permeability and separation performance of various binary systems (e.g., alcohol-hexane, alkane-hexane, diesel fuel-kerosene, and lipid-hexane systems) using the PDMS-based dense membrane.

Based on the important conclusions from the first part of this work, a new semi-empirical solution-diffusion model allowing the prediction of the solvent separation behavior in SRNF will be introduced for the first time.

2. Development of the new model

2.1 Assumptions

From the experimental results of Part A, to ensure preferential solvent transfer, some previous hypothesis should be complied with as follows.

1) The membrane should be a reverse osmosis (RO)-like one with a highly dense top layer and a possible void-free sublayer, so that the permeation happens through dissolving in the solid membrane surface and diffusing in the free volume in the membrane polymer chains. In other words, the transport mechanism should be a typical solution-diffusion one. The selectivity of DuraMem^{TM} 150 for ethanol/hexane and the SEM picture of it in Part A confirmed this assumption.
2) According to Equation (2) and (3) in Part A, strong interaction between one component and the membrane is necessary for separation, which means that membrane swelling could happen. If swelling happens, a pore-like structure may appear at the membrane surface and voids may form in the sublayer, which will lead to convective or viscous transport that weakens the selectivity due to coupled diffusion of solvent mixtures [4]. Therefore, the dominating mass transfer process for solvent separation in SRNF should be a solution-diffusion one even if swelling occurs.
3) It was found that only two factors, i.e. the Hansen solubility parameter and polarity, mostly mattered in the separation operation. Some other factors, like viscosity and surface tension, could be deleted from the model.
4) For smaller differences in Hansen solubility parameter and dielectric constant between one component and the membrane were, and simultaneously the larger those between one component and the other were, the more effective separation could be expected.

2.2 Model development

According to above assumptions, it is easy to infer that only the solution and diffusion parts of mass transfer should be taken into account, and the convection can be neglected. As a result, the total flux was as follows.

$$J_{Total\ flux} \propto A \tag{6}$$

The solvent permeability coefficient *A* was dependent on two factors, as the fourth assumption stated. Accordingly the solvent permeability coefficient should be expressed as:

$$A \propto \frac{1}{\Delta\sigma_{im}\Delta\varepsilon_{im}} \tag{7}$$

In Equation (7), $\Delta\sigma_{im}$ *and* $\Delta\varepsilon_{im}$ denote the difference in Hansen solubility parameter and dielectric constant between the solvent and membrane, respectively. According to Hansen's theory [17], $\Delta\sigma_{im}$ *was revised in the following form:*

$$\Delta\sigma_{im} = \left|\sigma_i^2 - \sigma_m^2\right|^{1/2} \tag{8}$$

With regard to polarity, the polarity by means of dielectric constant was given in Reference [18]. However, it is obvious that the calculated value of dielectric constant of polymers is often too low compared with that of solvents. For instance, polyvinyl alcohol, with a dielectric constant of 5.5, is a strong polar polymer, showing a high affinity toward water and a poor affinity toward alkanes. But the difference in dielectric constant between polyvinyl alcohol and water is about 72.5, which is far larger than that between polyvinyl alcohol and alkanes (about 3.5). Similar situation exists in the DuraMem™ and StarMem™ series membranes that are made from P84 polyimide and a blend of P84 and Matrimid 5218 [19-22], and so does MPF 44 that is made from polydimethylsiloxane (PDMS) [23]. If a simple form of direct dielectric constant difference was adopted, it was not able to reflect the real affinity between the membrane and solvent in a mathematical way. Consequently, to resolve this contradiction, $\Delta\varepsilon_{im}$ was revised as

$$\Delta\varepsilon_{im} = |\varepsilon_i - \varepsilon_m^3| \tag{9}$$

In summary, the flux of component i and j were expressed as

$$J_i \propto \frac{1}{|\varepsilon_i - \varepsilon_m^3| |\sigma_i^2 - \sigma_m^2|^{1/2}} \tag{10}$$

$$J_j \propto \frac{1}{|\varepsilon_j - \varepsilon_m^3| \left|\sigma_j^2 - \sigma_m^2\right|^{1/2}} \tag{11}$$

Combining Equation (10), (11) and Equation (5) in Part A, and molar ratio of compositions in the feed is 1:1. The resultant separation factor was expressed in Equation (12).

$$\alpha_{ij} = K \frac{|\varepsilon_j - \varepsilon_m^3|}{|\varepsilon_i - \varepsilon_m^3|} \sqrt{\frac{\left|\delta_j^2 - \delta_m^2\right|}{|\delta_i^2 - \delta_m^2|}} \tag{12}$$

In this equation K is a constant representing some intrinsic properties of the membrane, and the detailed derivation of α_{ij} was listed in Appendix A.

3. Experimental

All the relevant experimental separation factors, solvent properties were in Part A of this work, and further adopted to obtain information about the transport mechanism. The accurate solubility parameters and dielectric constant of these membranes are unknown due to patent protection, but according to their material, approximate values of them are available as listed in Table 1. Thus, the newly developed model and experimental data were implemented in mathematical computing software (Spss 13.0) and a least square fit was used to obtain the values of the unknown parameters (*K*) in Equation (12).

Table 1

4. Results and discussion

Figure 1-4

Figure 1-5 show the experimental data and the results of the different model fits. To validate the effectiveness of this model, only some experimental data (orange columns in Figure 1-4) were used to obtain the values of *K*, and the resultant model was adopted to predict separations factors of the other experimental data (grey columns in Figure 1-4). It is quite clear that the newly developed model describes the experimental data of DuraMem^{TM} 150, 200, 300 and MPF-44 satisfactorily, the values of R^2 for which are 0.763, 0.978, 0.997 and 0.994, respectively. DuraMem^{TM} 150 is the densest membrane possible within all membranes used, and the highest value of separation factor of all was found for ethanol/hexane. For other solvent pairs, although no obvious separation found, this new model still predicts well, which again proves the practicability of it from another perspective. As far as MPF 44 and DuraMem^{TM} 300 are concerned, they are also treated as dense membranes, for their MWCO is 200 and 300 Dalton, respectively. The main transport mechanism is supposed to follow the solution-diffusion mechanism, which has ever been confirmed by Geens et al. [7]. Corresponding to DuraMem^{TM} 200 with a value of R^2 equal to 0.4581, the MWCO of this membrane is 200 Dalton and the experimental data should be well related with the new model. The reason why this irregular phenomenon took place may be due to the mixture of methanol and CCl_4. During the permeation of this group of solvents, the color of the retentate was light yellow, which hinted that this membrane might lose its original property in contact with CCl_4. By removing the data of methanol/ CCl_4, the value of R^2 becomes 0.8709, indicating the usefulness of this model.

Figure 5

From Figure 5A and 5B, it can be seen that this model shows a very poor correlation with the StarMem^{TM} series membranes, despite that the MWCO of which are 220 and 400, respectively. The most possible reason may be the value of the dielectric constants of these two membranes. The StarMem^{TM} series membranes are made from P84 polyimide and a blend of P84 and Matrimid 5218 [19-22], and the dielectric constants of these two kinds of polyimide are 3.3 and 3.8, respectively [11]. When performing model fitting, choosing the right values of dielectric constant of them seems very difficult. What's more, these two membranes are commercial patent-protected products whose accurate properties are unknown, which may lead to the invalidation of the new model.

The poor fitting results of DuraMem^{TM} 500 and 900 in Figure 5C and Figure 5D are in line with the assumptions of this model. These two membranes are undoubtedly porous membranes with MWCO of 500 and 900, respectively. It means that a lot of pore-like structure and voids may exist in the membrane structure, which decides that the convection or viscous flow in the mass transfer of these membranes may play a leading role. For DuraMem^{TM} 500, the solution-diffusion transport might still help solvent permeation. Corresponding to DuraMem^{TM} 500, the value of R^2 reaches 8E-05, which implies that the solution-diffusion mechanism is totally not suitable for solvent transport through this loose SRNF membrane.

5. Conclusion

This work, for the first time, presents a semi-empirical model for describing solvent separation process in SRNF. The new model is only dependent on two factors, i.e. the Hansen solubility parameter and dielectric constant, combination of which provides a better way of characterize interactions between the solvent and membrane, or between binary solvent mixtures.

The model was evaluated with a large database of experimental separation factor data for a series of binary mixtures through different commercially available SRNF membranes. Statistical analysis was applied. For dense SRNF membranes, the model shows a high correlation except for the StarMem^{TM} series whose accurate relevant properties are unavailable. For loose membranes like DuraMem^{TM} 500 and 900, the model loses its applicability, which is in accordance with assumptions of the model.

This two paper series systematically investigate the separation performance of SRNF membranes for binary solvent mixtures. An interesting result was discovered for the permeation of ethanol/hexane through DuraMem^{TM} 150. Some important hypotheses which may allow the separation of solvent mixtures in SRNF have been put forward, and the most significant factors influencing this process were indentified. An instructive semi-empirical model based on the solution-diffusion mechanism was developed and its validation was confirmed using the experimental results. This work provides a new perspective for scientists in the field of SRNF, and further investigation into this process using high flux tailor-made membranes with clear physical and chemical properties should be carried out.

Acknowledgements

The Ministry of Finance and the Ministry of Education is gratefully acknowledged for their financial support to the central universities for fundamental research and to this work (Finance and Education, 173, 2009).

References

1. P. Vandezande, L. E. M. Gevers and I. F. J. Vankelecom, *Chem Soc Rev*, 2008, **37**, 365-405.
2. D. R. Machado, D. Hasson and R. Semiat, *J Membrane Sci*, 1999, **163**, 93-102.
3. J. Geens, K. Peeters, B. Van der Bruggen and C. Vandecasteele, *J Membrane Sci*, 2005, **255**, 255-264.
4. S. Darvishmanesh, J. Degrève and B. Van der Bruggen, *Chem Eng Sci*, 2009, **64**, 3914-3927.
5. D. R. Machado, D. Hasson and R. Semiat, *J Membrane Sci*, 2000, **166**, 63-69.
6. D. Bhanushali, S. Kloos, C. Kurth and D. Bhattacharyya, *J Membrane Sci*, 2001, **189**, 1-21.
7. J. Geens, B. Van der Bruggen and C. Vandecasteele, *Sep Purif Technol*, 2006, **48**, 255-263.
8. S. Darvishmanesh, A. Buekenhoudt, J. Degrève and B. Van der Bruggen, *J Membrane Sci*, 2009, **334**, 43-49.
9. S. Darvishmanesh, A. Buekenhoudt, J. Degrève and B. Van der Bruggen, *Sep Purif Technol*, 2009, **70**, 46-52.
10. A. Miyagi, H. Nabetani and M. Nakajima, *Sep Purif Technol*, 2012, **88**, 216-226.
11. D. Fierro, A. Boschetti-de-Fierro and V. Abetz, *J Membrane Sci*, 2012, **413**, 91-101.
12. P. Marchetti, A. Butté and A. G. Livingston, *J Membrane Sci*, 2012, **415**, 444-458.
13. P. Schmidt, T. K Se and P. Lutze, *J Membrane Sci*, 2013, **429**, 103-120.
14. P. Schmidt and P. Lutze, *J Membrane Sci*, 2013, **445**, 183-199.
15. L. Hesse, J. Mićović, P. Schmidt, A. Górak and G. Sadowski, *J Membrane Sci*, 2013, **428**, 554-561.
16. J. G. Wijmans and R. W. Baker, *J Membrane Sci*, 1995, **107**, 1-21.
17. D. J. Hansen C. M., *Hansen Solubility Parameters- A User's Handbook*, second edn., CRC Press, New York, 2007.
18. S. Darvishmanesh, J. Degrève and B. Van der Bruggen, *Chemphyschem*, 2010, **11**, 404-411.
19. Y. H. See Toh, X. X. Loh, K. Li, A. Bismarck and A. G. Livingston, *J Membrane Sci*, 2007, **291**, 120-125.
20. Y. H. See-Toh, F. C. Ferreira and A. G. Livingston, *J Membrane Sci*, 2007, **299**, 236-250.
21. E. Drioli and L. Giorno, *Comprehensive Membrane Science and Engineering*, Elsevier Science, 2010.
22. I. D. Wilson, E. R. Adlard, M. Cooke and C. F. Poole, *Encyclopedia of separation science*, Academic, 2000.
23. J. E. Mark, *Polymer Data Handbook*, Oxford University Press, Incorporated, 1999.

$J_{solvent}$-*solvent flux (L/hm^{2}bar^{-1})*

A- solvent permeability coefficient (L/m^{2}Pa)

v_m-solvent molar volume (cm^3/mol)

μ-*solvent viscosity (*mPa·s)

ϕ^n- a sorption value of solvent in the membrane （g/g polymer）

γ_{sv}- surface energy of the membrane (mN/m)

Δ_γ- difference in surface tension between the solid membrane material and the liquid solvent (mN/m)

D-diffusion coefficient [m^2/h]

$\Delta\pi$- osmotic pressure [Pa]

Δp-transmembrane pressure [Pa]

λ- membrane thickness (m)

ϕ_{mem}- volume fraction of membrane polymer in membrane phase [-]

σ_s- solubility parameter of solvent MPa$^{1/2}$

$J_{Total\ flux}$-*total solvent flux (L/hm^{2}bar^{-1})*

$\Delta\sigma_{im}$-difference in Hansen solubility parameter between the solvent and membrane (MPa$^{1/2}$)

$\Delta\varepsilon_{im}$-difference in dielectric constant between the solvent and membrane

σ_i- solubility parameter of component i (MPa$^{1/2}$)

σ_j- solubility parameter of component j (MPa$^{1/2}$)

σ_m-solubility parameter of the membrane (MPa$^{1/2}$)

ε_m- dielectric constant of the membrane

ε_i- dielectric constant of component i

ε_j- dielectric constant of component j

K-a constant representing some intrinsic properties of the membrane

α_{ij}- separation factor for the component i and j

Figure captions

Figure 1 Modelling of the separation factors of a series of binary solvent mixtures through a DuraMem^{TM} 150 membrane. Orange columns：experimental data for model fitting; grey columns: experimental data; dark green columns: model data.

Figure 2 Modelling of the separation factors of a series of binary solvent mixtures through a DuraMem^{TM} 200 membrane. Orange columns：experimental data for model fitting; grey columns: experimental data; dark green columns: model data.

Figure 3 Modelling of the separation factors of a series of binary solvent mixtures through a DuraMem^{TM} 300 membrane. Orange columns：experimental data for model fitting; grey columns: experimental data; dark green columns: model data.

Figure 4 Modelling of the separation factors of a series of binary solvent mixtures through a MPF-44 membrane. Orange columns： experimental data for model fitting; grey columns: experimental data; dark green columns: model data.

Figure 5 Modelling of the separation factors of a series of binary solvent mixtures through StarMem^{TM} 122, StarMem^{TM} 240, DuraMem^{TM} 500, DuraMem^{TM} 900 membranes.

Figure 1

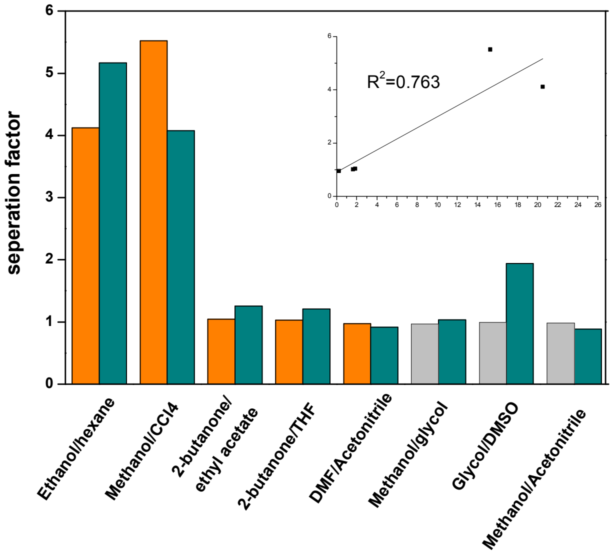
seperation factor
0
1
2
3
4
5
6
Ethanol/hexane
Methanol/CCl4
2-butanone/ ethyl acetate
2-butanone/THF
DMF/Acetonitrile
Methanol/glycol
Glycol/DMSO
Methanol/Acetonitrile
R^2=0.763
0
2
4
6
0
2
4
6
8
10
12
14
16
18
20
22
24
26

Figure 2

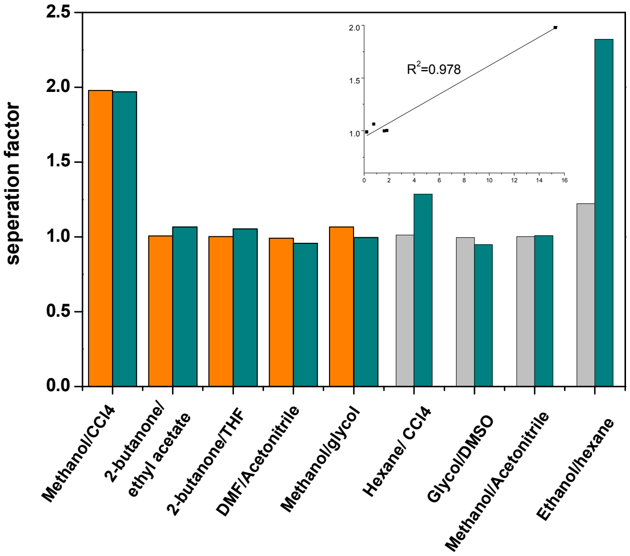
seperation factor
2.5
2.0
1.5
1.0
0.5
0.0
Methanol/CCl4
2-butanone/
ethyl acetate
2-butanone/THF
DMF/Acetonitrile
Methanol/glycol
Hexane/ CCl4
Glycol/DMSO
Methanol/Acetonitrile
Ethanol/hexane
R2=0.978
2.0
1.5
1.0
0
2
4
6
8
10
12
14
16

Figure 3

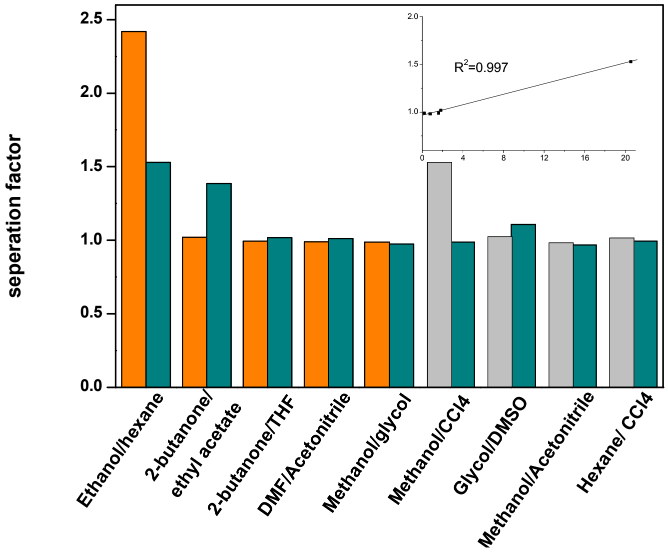
seperation factor
0.0
0.5
1.0
1.5
2.0
2.5
Ethanol/hexane
2-butanone/
ethyl acetate
2-butanone/THF
DMF/Acetonitrile
Methanol/glycol
Methanol/CCl4
Glycol/DMSO
Methanol/Acetonitrile
Hexane/ CCl4
R^2=0.997
2.0
1.5
1.0
0
4
8
12
16
20

Figure 4

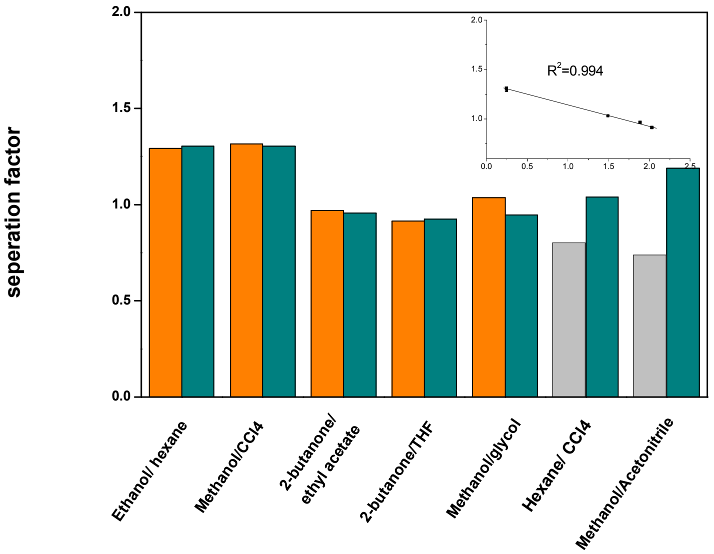
seperation factor
2.0
1.5
1.0
0.5
0.0
2.0
1.5
1.0
R^2=0.994
0.0
0.5
1.0
1.5
2.0
2.5
Ethanol/ hexane
Methanol/CCl4
2-butanone/ ethyl acetate
2-butanone/THF
Methanol/glycol
Hexane/ CCl4
Methanol/Acetonitrile

Figure 5

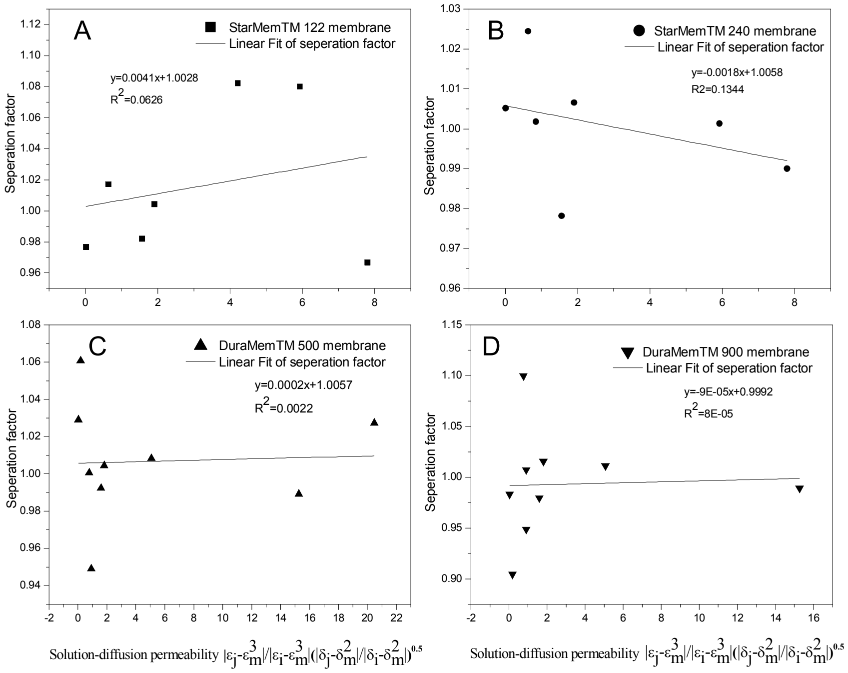
A
■ StarMemTM 122 membrane
Linear Fit of seperation factor
y=0.0041x+1.0028
R^2=0.0626
Seperation factor
0.96 0.98 1.00 1.02 1.04 1.06 1.08 1.10 1.12
0 2 4 6 8
B
● StarMemTM 240 membrane
Linear Fit of seperation factor
y=-0.0018x+1.0058
R2=0.1344
Seperation factor
0.96 0.97 0.98 0.99 1.00 1.01 1.02 1.03
0 2 4 6 8
C
▲ DuraMemTM 500 membrane
Linear Fit of seperation factor
y=0.0002x+1.0057
R^2=0.0022
Seperation factor
0.94 0.96 0.98 1.00 1.02 1.04 1.06 1.08
-2 0 2 4 6 8 10 12 14 16 18 20 22
Solution-diffusion permeability $|\varepsilon_j-\varepsilon_m^3|/|\varepsilon_i-\varepsilon_m^3|(|\delta_j-\delta_m^2|/|\delta_i-\delta_m^2|)^{0.5}$
D
▼ DuraMemTM 900 membrane
Linear Fit of seperation factor
y=-9E-05x+0.9992
R^2=8E-05
Seperation factor
0.90 0.95 1.00 1.05 1.10 1.15
-2 0 2 4 6 8 10 12 14 16
Solution-diffusion permeability $|\varepsilon_j-\varepsilon_m^3|/|\varepsilon_i-\varepsilon_m^3|(|\delta_j-\delta_m^2|/|\delta_i-\delta_m^2|)^{0.5}$

Table captions

Table 1 The values of solubility parameter and dielectric constant of membranes used in this work

Table 1

Membrane Type	Material	Solubility parameter (MPa$^{1/2}$)	Dielectric constant
The StarMem^{TM} series	Polyimide	23.2 [19]	3.3~3.8 [13]
The DuraMem^{TM} series	Modified polyimide	26.8 [19]	3.3 [13]
MPF-44	PDMS	15.5 [20]	2.3-2.8 [18]